K. Yamada, M. G. Kim,* and T. Kunio**

Tolerant Microflaw Sizes and Non-Propagating Crack Behaviour

REFERENCE Yamada, K., Kim, M. G., and Kunio, T., **Tolerant Microflaw Sizes and Non-Propagating Crack Behaviour,** *The Behaviour of Short Fatigue Cracks*, EGF Pub. 1 (Edited by K. J. Miller and E. R. de los Rios) 1986, Mechanical Engineering Publications, London, pp. 261–274.

ABSTRACT The critical length of non-propagating cracks in plain carbon steel specimens with three different carbon contents of 0.36%C, 0.55%C, and 0.84%C are compared with the critical size of artificially induced micropits prepared by electro-discharge-machining in order to discuss the physical meaning of the endurance limit and the evaluation of the tolerant microflaw size at the stress level of the endurance limit.

It is found that there exists a particular size of micropit below which there is no effect on the endurance limit. This critical size of micropit can be regarded as equivalent to a tolerant microflaw which would not reduce the endurance limit.

It is also found that this critical micropit size does not necessarily coincide with the critical length of a non-propagating crack but coincides with the critical length of an annealed pre-crack.

Local residual stress around artificially introduced microflaws are cited as the reason for discrepancies when compared to natural cracks in plain un-notched specimens.

Introduction

It is well known that the endurance limit of plain carbon steel smooth specimens corresponds to the critical stress for the onset of growth of non-propagating cracks(NPCs), but does not correspond to the critical stress for the initiation of such a crack (**1**)(**2**). The appearance of a NPC in a fatigued specimen implies the possible existence of a tolerant flaw which would not reduce the original endurance limit.

Murakami and others (**3**)–(**5**) have made a comprehensive study of the relationship between the size of a NPC and an artificial micropit size. However, difficulties in finding the critical size of a crack, namely, the maximum size of a NPC in a smooth specimen (**2**), has perturbed a proper understanding of the relationship between the size of a NPC and the tolerant flaw size.

The authors have recently reported that the critical size of NPCs in plain carbon steel grow up to a length ranging from 200 μm to 300 μm during stage II growth, which is equivalent to several orders of magnitude greater than the matrix ferrite grain size (**2**)(**6**), and also that the non-propagation of such cracks can result from the closure associated mainly with localized residual compressive stresses which are produced around the crack tip during fatigue loading (**7**).

Fatigue loading history also has an influence on the critical size of a NPC. Even a large crack which would not become a NPC under a conventional stress

* Department of Mechanical Engineering, Keio University 3-14-1 Hiyoshi, Kohoku-ku, Yokohama 223, Japan.

amplitude at the endurance limit, can become a NPC under the same stress level if the crack tip is changed from an open state to a closed state by coaxing effects (7)(8). This evidence may suggest that loading history may have an important role on the critical size of a NPC and that the tolerant flaw size is not directly related to the size of a NPC. It may be said therefore that there still remain some uncertainties in characterizing the critical size of a NPC; a requirement in evaluating the level of the endurance limit from a mechanistic viewpoint.

In this paper special emphasis is placed on the nature of NPCs and the size of tolerant flaws when considering the relationship between the critical size of a micropit and a NPC in plain carbon steel specimens subjected to constant stress amplitude.

Materials and experimental methods

The materials used in this experiment are plain carbon steels with three different carbon contents as given in Table 1. This table also shows the heat treatment condition for each material. These materials were machined into solid hourglass shape specimens having a 9 mm diameter and a 20 mm radius of curvature at the gauge length so as to make microscopic observation easy. Details of the specimen are given in Fig. 1. The stress concentration factor of this geometry is about 1.06, so that these specimens may be regarded as smooth test pieces.

Every specimen was vacuum-annealed at 640°C for 1 hour and then electro-polished by approximately 10 μm in depth in order to eliminate residual stresses and strains due to machining. Rotating bending fatigue tests were carried out on these specimens at a frequency of 48 Hz.

Mechanical properties and microstructural parameters of the specimens are given in Table 2. Volume fraction of pearlite and ferrite grain size were measured by the line counting method (9). A micro-Vickers indentor was selected with a 20 g and 50 g mass for the ferrite and pearlite grains, respectively. Micrographs of the surface microstructure of each specimen are given in Fig. 2. The white portion in the micrograph of the 0.84%C specimen represents the ferrite phase which has decarburized due to the high temperature annealing at 1200°C; the volume fraction of this ferrite is 6 per cent of the

Table 1 Chemical composition and heat treatments of materials

Chemical composition wt%	0.84%C-Steel	C:0.84 Si:0.22 Mn:0.45 P:0.014 S:0.027 Cu:0.03 Ni:0.02Cr:0.10
	0.55%C-Steel	C:0.55 Si:0.22 Mn:0.69 P:0.017 S:0.021
	0.36%C-Steel	C:0.36 Si:0.27 Mn:0.53 P:0.014 S:0.011
Heat treatment condition	0.84%C-Steel	1200°C 2 hr annealing
	0.55%C-Steel	810°C 2 hr annealing
	0.36%C-Steel	1000°C 2 hr annealing

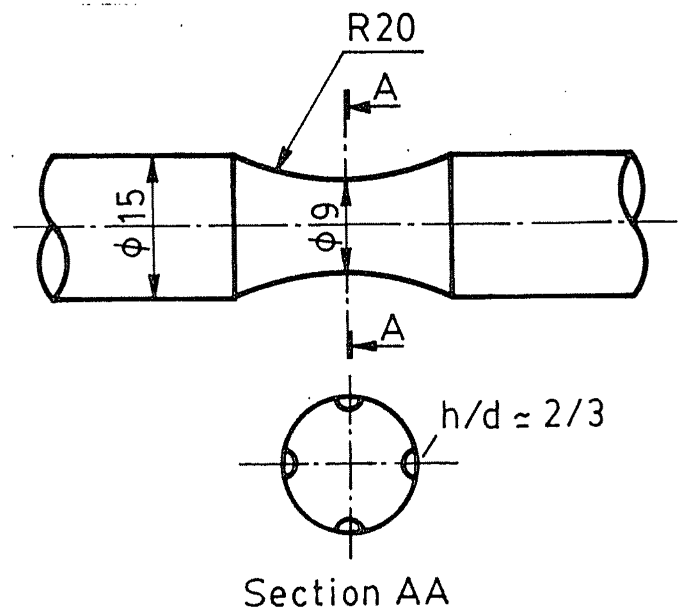

Fig 1 Details of specimen geometry and a schematic illustration of the position of micropits

surface microstructure. Some specimens then had four artificial micropits introduced as shown in Fig. 1, with axial symmetry, on their surface. Micropits may be considered as microflaws in the material and they were inserted by electro-discharge-machining (EDM) and had a dimensional ratio of $h/d \simeq 2/3$ where d and h are the diameter and the depth, respectively. The measurement of crack length was by an optical microscope and was determined in a direction perpendicular to the specimen axis.

The endurance limit of each specimen was determined experimentally as the maximum stress, below which the specimen will not fracture after a repetition of 10^7 stress cycles. Approximately 10 specimens were used to determine each endurance limit.

Table 2 Mechanical properties and microstructural parameters of three materials

Specimen	*0.84%C Steel*	*0.55%C Steel*	*0.36%C Steel*
Volume fraction of pearlite (%)	94	71	45
Ferrite grain size (μm)	—	5	26
Micro-vickers hardness of ferrite	150	132	142
Micro-vickers hardness of pearlite	257	239	247
0.2% proof stress (MPa)	277	314	184
Ultimate tensile strength (MPa)	714	649	512
Endurance limit (MPa)	210	245	194

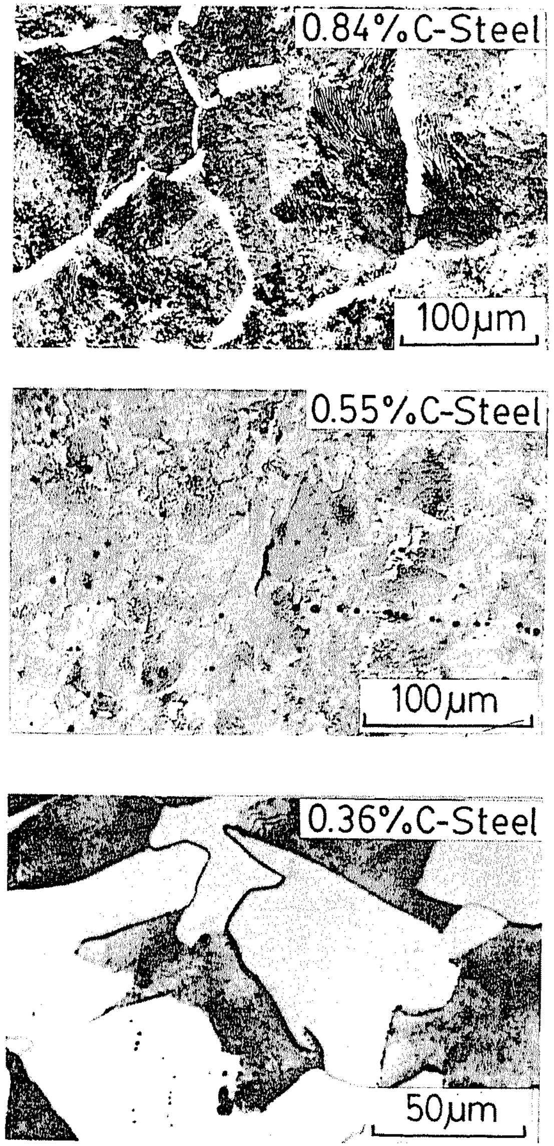

Fig 2 Surface microstructure of specimens

Results and discussion

An estimation of the critical size of a tolerant microflaw

The endurance limits, σ_e, of smooth specimens obtained from rotating bending fatigue tests are 210 MPa, 245 MPa, and 194 MPa for 0.84%C, 0.55%C, and 0.36%C steel specimens, respectively.

Tests indicate that a relatively large NPC, of stage II growth, has grown to a length several orders of magnitude greater than the matrix ferrite grain size. Thus the existence of tolerant microflaws equivalent to the critical length of a NPC may be expected at the endurance limit.

In order to discuss the relationship between the length of a NPC and the size of a tolerant microflaw, the following experiment was carried out. Several 0.84%C steel specimens, with micropits ranging from 100 to 350 μm, were tested at 210 MPa, the original endurance limit of smooth specimens. Results are shown in Fig. 3 by a solid line with open symbols. This figure shows that the largest micropit diameter which does not cause a fatigue fracture at the endurance limit is approximately 230 μm. This particular size can be regarded

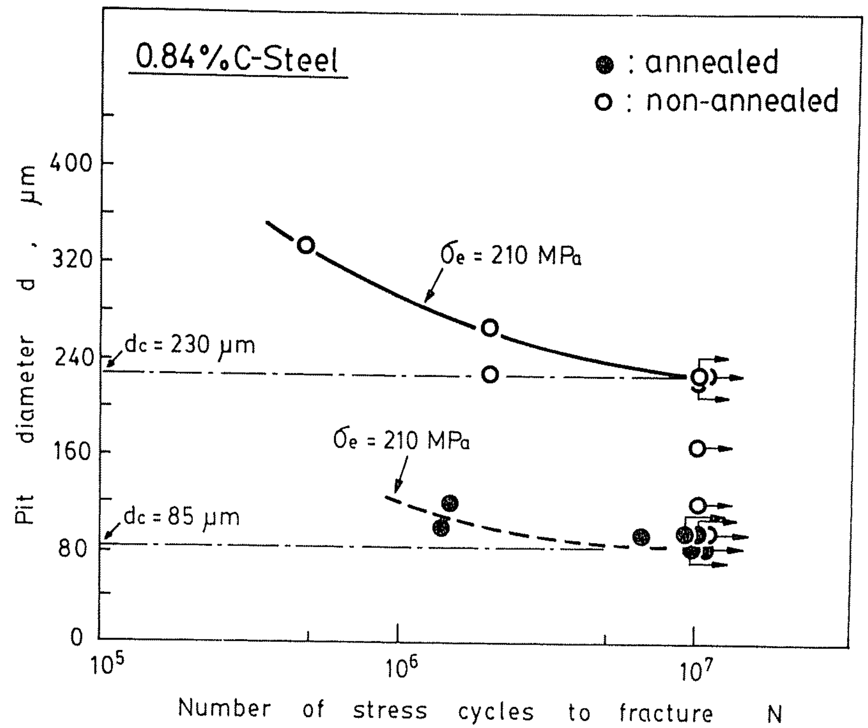

Fig 3 An evaluation of tolerant microflaws at the original endurance limit of σ_e = 210 MPa

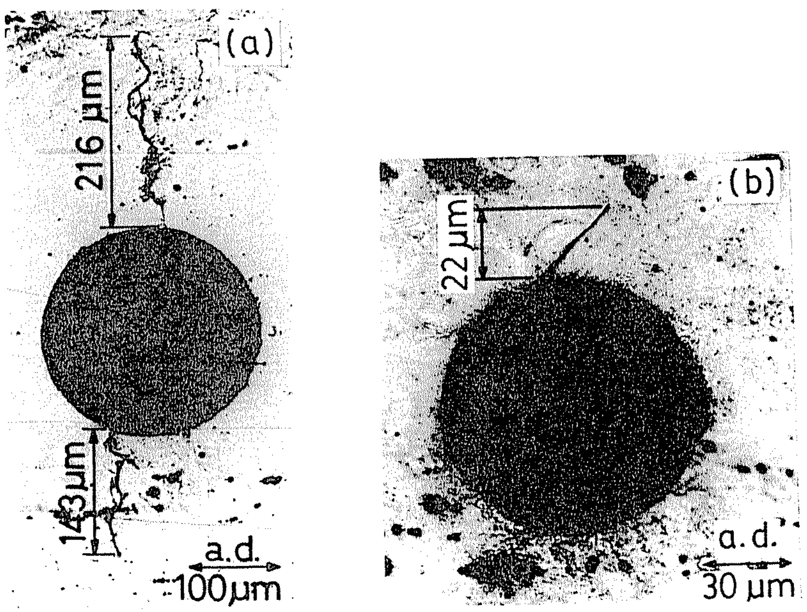

Fig 4 **(a) A NPC which initially propagated from the edge of a non-annealed EDM pit at $\sigma = 210$ MPa and $N = 10^7$ cycles**

(b) A NPC which initially propagated from the edge of an annealed EDM pit at $\sigma = 210$ MPa and $N = 10^7$ cycles

as the critical size of a tolerant microflaw which does not affect the original level of the endurance limit of this material.

Furthermore, it is found from microscopic observations around the pit that NPCs originated from pits and propagated to a length comparable with the pit size; see, for example, Fig. 4(a). This means that the condition for the onset of fatigue fracture cannot be determined by the critical stress to initiate a crack at the periphery of a pit, but must be determined by the critical stress to cause the growth of the NPC.

It should be noted that if we take 'pit diameter + NPC length' as an effective length of a NPC, the critical length of a NPC can be regarded as approximately 580 μm, which is fairly large compared with the critical length of a NPC on a smooth specimen, which was approximately 340 μm. A reason for the appearance of such a large NPC can be explained by the possible effects of residual compressive stress associated with localized plasticity at the crack tip during cyclic loading and also from the machining by EDM (**10**). To examine the effects of residual stress on the non-propagating behaviour of a crack, a particular specimen was used with a NPC of 200 μm length which had propagated from the edge of the pit thus giving an effective length of 400 μm.

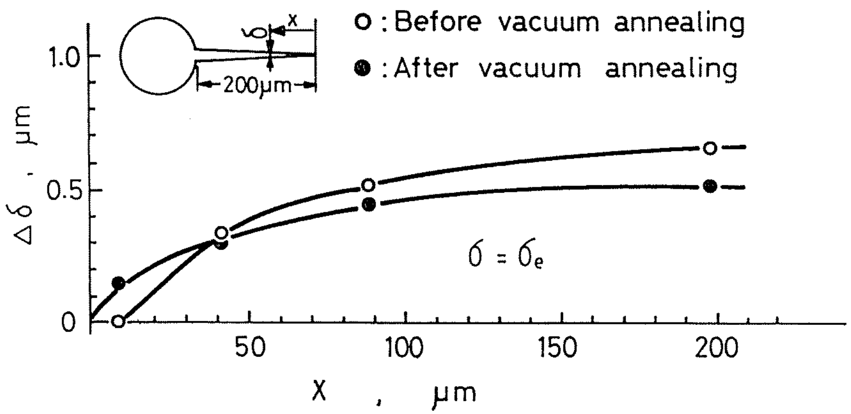

Fig 5 **The range of crack opening displacment of a NPC before and after vacuum annealing**

A stress relief annealing was performed in vacuum at 640°C for 1 hour, but after measurements of crack opening displacement were made using a method given in a previous study (**7**). Measurements of crack opening displacement were made again on the same crack after this heat treatment. Results are as shown in Fig. 5.

This figure explains that the crack tip of a NPC which was closed, opens after vacuum annealing under the application of a static bending stress equivalent to the endurance limit. Therefore it can be interpreted that the non-propagation behaviour of a crack nucleated from the pit is caused by closure effects (**11**)–(**14**) due mainly to residual compressive stresses in the same manner as ordinary NPCs. However, it is difficult to distinguish which residual stress is dominant, the residual stresses due to localized plasticity or that created in the process of making a pit.

Since an effect of residual stress around the pit cannot be negligible even in the case of an EDM pit(**10**), the critical size of a pit should be examined under experimental conditions excluding the effects of EDM residual stresses. Therefore, newly prepared specimens were all vacuum-annealed after EDM in order to provide specimens with pits free of residual stress. These specimens were fatigue tested at the stress level of the original endurance limit. Results are shown in Fig. 3. This figure shows the results of fatigue tests on two different types of specimen: the solid line with open symbols is for specimens having conventional EDM pits while the broken line with solid symbols is for specimens having pits free of residual stress. These results show that the critical size of a tolerant micropit decreases from 230 μm to 85 μm when the residual stress due to EDM is removed.

This value of 85 μm should be regarded as the tolerant microflaw size in this material rather than the conventional EDM micropit size of 230 μm.

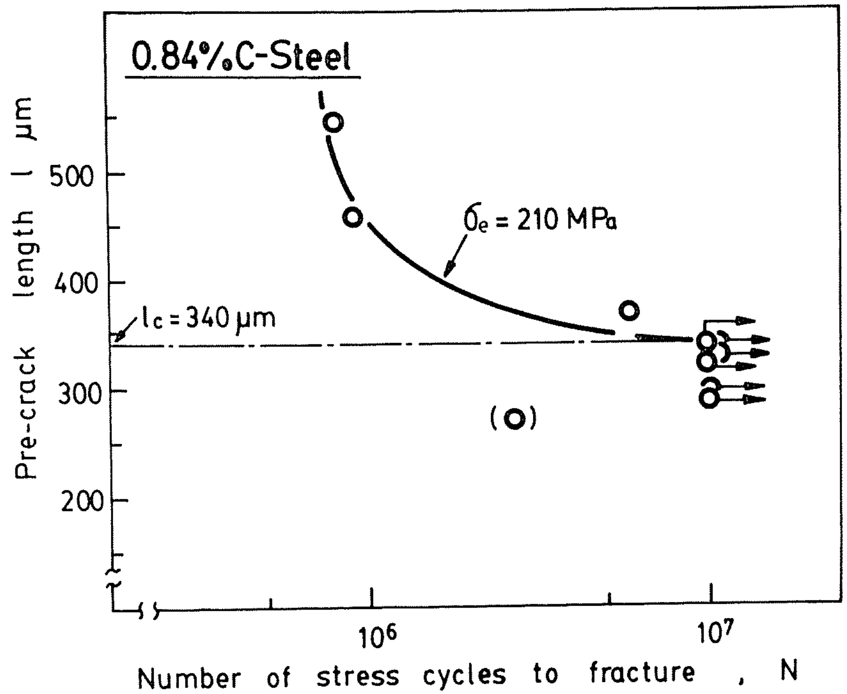

Fig 6 An evaluation of the critical size of a NPC from a fatigue pre-cracked specimen (7)
(O): fracture caused by a coalescence of neighbouring cracks

Relationship between the critical size of a tolerant microflaw and the critical NPC length of a smooth specimen

The critical length of a NPC of the present material was obtained as 340 μm as shown in Fig. 6, which the authors have already reported in a previous paper (7). This result indicates that the critical size of that micropit in this material, 85 μm, does not coincide with the critical NPC length of 340 μm obtained from pre-cracked specimens having various sizes of natural surface fatigue cracks in a smooth specimen.

Since a NPC in a plain specimen has resulted from the accumulation of cyclic loading effects, including crack tip closure, and the EDM micropit is free from any fatigue loading history, it is perhaps understandable that the results do not coincide.

As the above critical micropit size of 85 μm generates a NPC of 22 μm, as shown in Fig. 4(b), the effective crack length amounts to 85 + 22 μm; however, this is still much less than the critical NPC length of 340 μm.

Figure 6 provides data on un-annealed specimens and so it may be suggested that the fatigue pre-cracks should be subjected to annealing before fatigue

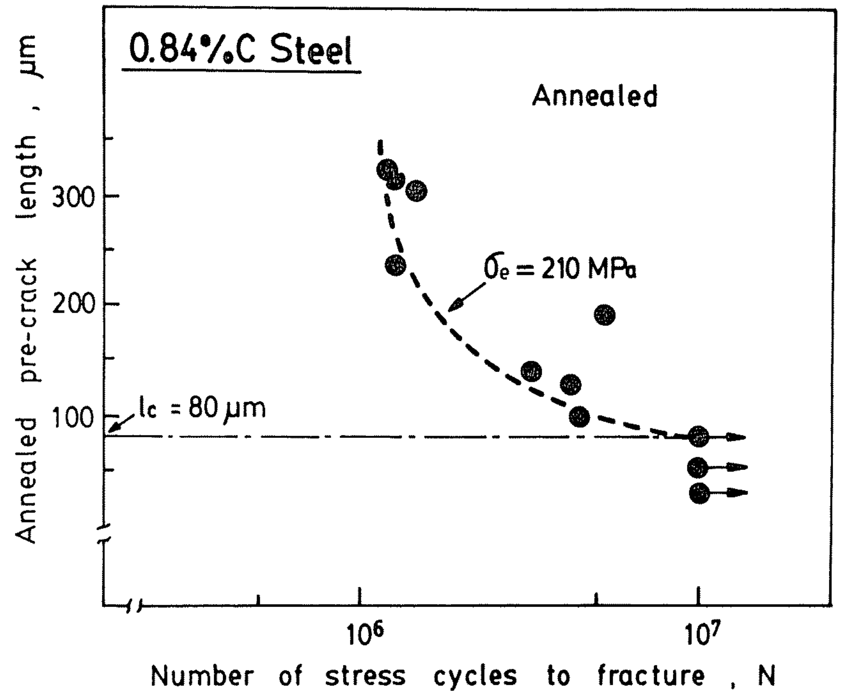

Fig 7 An evaluation of the critical length of an annealed pre-crack

testing. We have previously obtained this evidence by annealing at 640°C for 1 hour, after which the crack is no longer a NPC but a propagating crack at the stress level of the original endurance limit (7).

For the purpose of examining the change in the critical length due to annealing, specimens with a fatigue pre-crack were prepared at a stress level 10 per cent above the endurance limit. A desired length of fatigue pre-cracks can be obtained by stopping the fatigue test at a certain number of cycles prior to a vacuum-anneal at 640°C for 1 hour which makes the fatigue pre-cracks free of residual stress. These specimens were then fatigue tested at the stress level of the original endurance limit. Results are given in Fig. 7. This figure shows that the largest crack length, which will not fracture the specimen after 10^7 cycles of repetition at the stress equivalent to the original endurance limit, can be determined as approximately 80 μm.

The critical size of a micropit which is free from EDM residual stress, agrees well with this critical size from an annealed pre-cracked specimen.

In order to examine the generality of the above coincidence for a wide range of carbon content, two other kinds of specimen were used for similar fatigue experiments as those for the 0.84% C steel specimens. Results are given in Fig. 8.

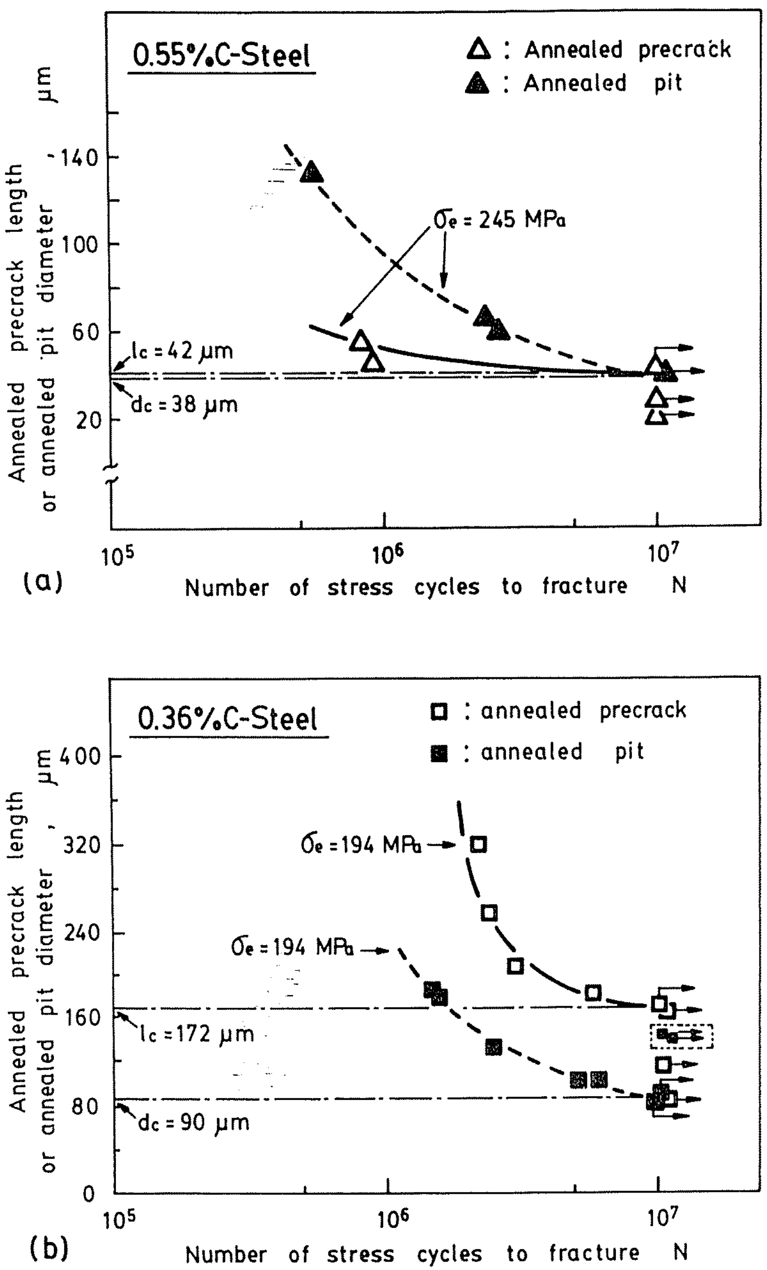

Fig 8 An evaluation of critical lengths

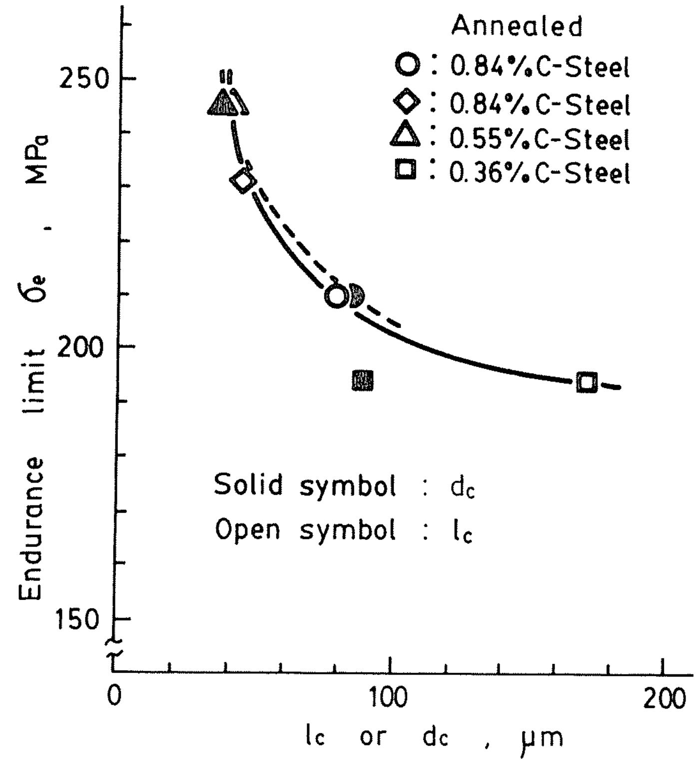

Fig. 9 Relationships between the endurance limit and defect sizes (micropits and plain specimen non-propagating cracks) in annealed steels
◇: unpublished work by the authors

In the case of the 0.55%C steel, good agreement is obtained; compare 42 μm and 38 μm, respectively. However, in the case of the 0.36%C steel a relatively poor agreement is recognized between 172 μm and 90 μm, respectively. These results, together with that of the 0.84%C specimen, are represented in Fig. 9.

In this figure, a solid line with open marks indicates the relationship between plain specimen data and σ_e while the broken line with solid marks indicates the relationship between the critical micropit size and σ_e. Both relationships show good agreement with each other for the two higher carbon contents, but in the case of the 0.36%C steel there is no agreement.

The disagreement in 0.36%C steel samples could be associated with the decrease in the volume fraction of pearlite, which acts effectively to suppress the crack propagation around the pit. Since the initiation and propagation of a crack is associated with the local volume fraction of pearlite around the pit rather than the average volume fraction, we may expect good agreement between the two parameters in the 0.36%C steel if the local volume fraction

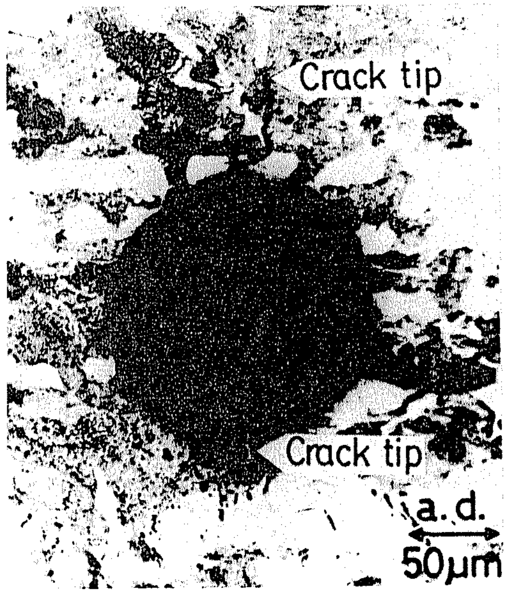

Fig 10 The 144 μm diameter EDM pit which lies within the locally high carbon domain of the 0.36%C steel specimen and the short non-propagating crack which is impeded in its propagation by the surrounding pearlitic structure; $\sigma = 194$ MPa, $N = 10^7$ cycles

around the pit is pre-arranged by choosing a location of the EDM pit within a pearlite colony.

On the basis of this consideration, two specimens were prepared having annealed pits of 140 μm and 144 μm diameters. These pits lie within a locally high carbon domain as shown in Fig. 10. These specimens were then tested at the endurance limit of 194 MPa. These specimens did not fail after 10^7 stress cycles as expected. The two results are shown surrounded by a broken line inset in Fig. 8(b). Thus it is found that the critical micropit size changes from 90 to at least 144 μm when the microstructure surrounding the pit is changed from a mixture of pearlite and ferrite to one of pearlite.

It may be concluded that the critical size of a micropit is closely associated with the local state of mixture of pearlite and ferrite around the pit rather than the average volume fraction of pearlite, i.e., the difference of crack growth resistance between the pearlite and ferrite constituents.

Conclusions

Studies have been performed on the physical meaning of the endurance limit and the tolerant microflaw size of plain carbon steel specimens with three different carbon contents.

The results are summarized as follows.

(1) There exists a particular size of artificial micropit which would not alter the original level of the endurance limit in plain carbon steel specimens. This particular size of micropit can be regarded as the critical size of a tolerant microflaw which would not reduce the original level of the endurance limit.

(2) The critical size of an artifically induced micropit does not necessarily coincide with the length of a non-propagating crack due to micro-residual stress effects in the former and different crack closure histories of the latter. Annealing of both types of specimen provides better agreements.

(3) A local residual stress around the micropit apparently increases the size of the critical tolerant microflaw size.

(4) The critical size of an artificial micropit in a plain carbon steel is influenced by the local volume fraction of pearlite around the pit rather than the average volume fraction.

Acknowledgement

The authors would like to thank Professor M. Shimizu for his valuable discussion and encouragement.

References

(1) KUNIO, T., SHIMIZU, M., and YAMADA, K. (1969) Microstructural aspects of the fatigue behaviour of rapid heat-treated steel, *Proceedings of the 2nd International Conference on Fracture* (Chapman & Hall, London), pp. 630–642.

(2) KUNIO, T. and YAMADA, K. (1979) Microstructural aspects of the threshold condition for the non-propagating fatigue cracks in martensitic and ferritic steel, *ASTM STP* 675, 342–370.

(3) MURAKAMI, Y., FUKUDA, S., and ENDO, T. (1978) Effect of micro-hole on fatigue strength: (1st Report) Effect of micro-hole of 40 μm–200 μm in diameter on the fatigue strength of annealed 0.13% and 0.46% carbon steel, *Trans. Jap. Soc. mech. Engrs*, **44**, 4003–4013.

(4) MURAKAMI, Y., KAWANO, H., and ENDO, T. (1979) Effect of micro-hole on fatigue strength: (2nd Report) Effect of micro-hole of 40 μm–200 μm in diameter on the fatigue strength of quenched and tempered 0.46% carbon steel, Loc. cit. **45**, 1479–1486.

(5) MURAKAMI, Y., TAZUNOKI, Y., and ENDO, T. (1981) Existence of coaxing effect and effect of small artificial holes of 40 μm–200 μm diameter on fatigue strength in 2017S-T4 Al alloy and 7:3 Brass, Loc. cit. **47**, 1293–1300.

(6) KUNIO, T., SHIMIZU, M. YAMADA, K., and TAMURA, M. (1984) Endurance limit and threshold condition for microcrack in steel, *Proceedings of the 2nd International Conference on Fatigue and Fatigue Thresholds,* Birmingham, UK, pp. 817–826.

(7) KUNIO, T., YAMADA, K., and KIM, M. G. (1984) Critical behaviour of non-propagating crack in steel, *Proceedings of the International Symposium on Fundamental Questions and Critical Experiments on Fatigue*, ASTM, Dallas, USA.

(8) KIM, M. G., YAMADA, K., and KUNIO, T. (1985) Effect of cyclic stress history on the threshold condition for microcrack in structural steel, *Trans. Jap. Soc. mech. Engrs*, **51**, 1529–1533.

(9) De HOFF, R. T. and RHINES, F. N. (1968) *Quantitative Microscopy* (McGraw-Hill, New York), pp. 55–59, 269–270 (Japanese Edition).

(10) *Technical Handbook of EDM* (1963), Nikkan Kogyo Shimbun Co., Japan, pp. 73–74.

(11) ELBER, W. (1971) The significance of fatigue crack closure, *ASTM STP 486*, pp. 230–242.

(12) SURESH, S., ZAMISKI, G. F., and RITCHIE, R. O. (1981) Oxide-induced crack closure: An explanation for near-threshold corrosion fatigue crack growth behaviour, *Met. Trans.* **12A**, 1435–1443.
(13) MINAKAWA, K. and McEVILY, A. T. (1981) On crack closure in the near-threshold region, *Scripta Met.*, **15**, 633–636.
(14) KOBAYASHI, H. (1982) Recent research on fatigue crack growth, *Bull. Jap. Inst. Metals*, **21**, 329–338.